LEICA: A Low Energy Ion Composition Analyzer for the Study of Solar and Magnetospheric Heavy Ions

Glenn M. Mason, Douglas C. Hamilton, Peter H. Walpole, Karl F. Heuerman, Tommy L. James, Michael H. Lennard, and Joseph E. Mazur

Abstract— **The SAMPEX LEICA instrument is designed to measure ~0.5–5 MeV/nucleon solar and magnetospheric ions over the range from He–Ni. The instrument is a time-of-flight mass spectrometer which measures particle time-of-flight over a ~0.5 m path, and the residual energy deposited in an array of Si solid state detectors. Large area microchannel plates are used, resulting in a large geometrical factor for the instrument (0.6 cm^2 sr) which is essential for accurate compositional measurements in small solar flares, and in studies of precipitating magnetospheric heavy ions.**

I. Introduction

THE composition of energetic particles accelerated in solar flares, interplanetary shocks, and magnetospheric storm and precipitation events carries information about the source region of the particles and the physical processes involved in their acceleration at the source site and subsequent transport to the observer. Since particle spectra from these events fall steeply with increasing energy, the composition can be most accurately studied at relatively low energies. The Low Energy Ion Composition Analyzer (LEICA) on the Solar, Anomalous, and Magnetospheric Particle Explorer (SAMPEX) mission is designed to investigate these low energy particles. LEICA is a time-of-flight mass spectrometer covering the energy range ~ 0.5-5 MeV/nucleon. The instrument measures ion mass, energy, and arrival direction for the range He–Ni (3–60 AMU).

The LEICA sensor is an evolution of a compact time-of-flight mass spectrometer developed for an interplanetary spacecraft [1], [2]. A full-sized version of the instrument was constructed for flight in a NASA "Get-Away-Special" canister, and, together with the Heavy Ion Large Telescope (HILT) sensor [3], flew on the space shuttle mission STS-28 in August 1989 [4], [5].

II. Scientific Objectives

A. Solar Energetic Particles

Solar flare events typically accelerate particles to energies of tens of MeV/nucleon, with occasional flares producing relativistic particles which are detectable by ground-based neutron monitors. In recent years, two broad classes of energetic particle events have been identified: large events which are characterized by high flux levels and acceleration time scales at the sun of tens of hours (e.g., [6], [7]), and small, impulsive events which are generally enriched in ^{3}He, heavy elements such as Fe, and electrons e.g., [8], [9]. Particle acceleration in large flares seems to be associated with large shocks near the sun, and their average abundances appear to be close to those in the solar corona (reviews by Mason [10], Lin [11]). In contrast, impulsive, small flares appear to accelerate particles at the much hotter flare site itself (e.g., review by Reames [12]).

Additional measurements of solar flare composition, energy spectra, and ionization state can therefore give new information on both the large and impulsive solar flare processes. When SAMPEX is at high geomagnetic latitudes, LEICA will sample solar energetic particles at the low energies where abundances are high enough to make accurate statistical measurements even in relatively small solar flares. At lower magnetic latitudes, the solar particles are excluded by the earth's magnetic field. By measuring the rigidities for which solar flare fluxes are cut off by the geomagnetic field, LEICA will yield information on the mean charge state of the solar flare ions, thus giving insights into, e.g., the temperatures of the originally accelerated material.

In addition to the elemental composition and energy spectra of solar energetic particles, LEICA will measure the isotopic composition over a limited range near 1 MeV/nucleon, thus supplementing the measurements to be performed by the Mass Spectrometer Telescope (MAST) sensor. The significance of the solar isotopic studies is described in the accompanying paper on the MAST instrument [13].

B. Magnetospheric Precipitating Heavy Ions and Energetic Neutrals

Magnetospheric heavy ions of energies near 0.5 MeV/nucleon were first reported by Van Allen *et al.* [14]; in particular, a number of observers discovered low altitude equatorial particles with origin in the ring current [15]–[18]. Scholer *et al.* [19] detected large fluxes of CNO during a geomagnetic storm using instruments on a low earth orbiting satellite (perigee ~ 230 km, apogee ~ 1500 km); more recently, Rassoul

Manuscript received August 3, 1992; revised January 19, 1993.

G. M. Mason, D. C. Hamilton, P. H. Walpole, K. F. Heuerman, T. L. James, M. H. Lennard, and J. E. Mazur are with the Department of Physics, University of Maryland, College Park, MD 20742.

G. M. Mason is also with the Institute of Physical Science and Technology, University of Maryland, College Park, MD 20742.

IEEE Log Number 9208074.

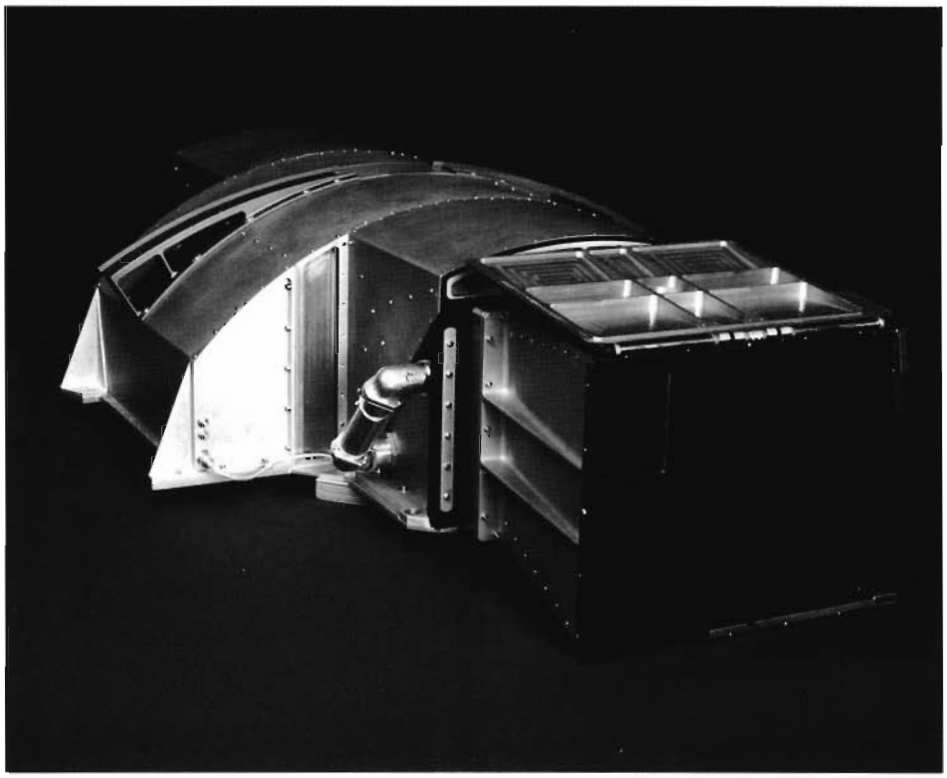

Fig. 1. The LEICA instrument shown with acoustic cover opened and thermal blankets removed. The arc-shaped raised fitting on the electronics box is a cable channel for the spacecraft despin yo-yos.

et al. [20] discussed the optical emissions associated with precipitation of heavy ions and energetic neutrals from the ring current. The CNO/He ratio of $\sim 5.5 \times 10^{-2}$ at 0.25 MeV/nucleon observed by Scholer *et al.* was consistent with either a solar wind or ionospheric origin, but they pointed out that a measurement of the C to O ratio could give a decisive test. The LEICA instrument on SAMPEX will measure many such events with detailed compositional information, making it possible to gain new insights into the dynamics of these magnetospheric particles.

III. Instrument Description

A. Sensor

The LEICA sensor identifies ion type and energy by simultaneously measuring the time-of-flight t and residual kinetic energy E of particles which enter the telescope and stop in one of an array of four Si solid state detectors. An overview of the flight instrument is shown in Fig. 1, and the instrument resource requirements are listed in Table I. Fig. 2 shows a simplified cross sectional view of the basic elements of the telescope sensor. The time-of-flight is determined from START and STOP pulses from chevron microchannel plate (MCP) assemblies which detect secondary electrons that are emitted from the entrance foil and from a foil in front of the solid state detectors when an ion passes through them. The measured energy $E = 1/2\ mv^2$ and the velocity $v = L/t$ (where L is the path length) are combined to yield the mass of the ion

$$m = 2E(t/L)^2 \tag{1}$$

TABLE I
LEICA Resources

Mass	7.43 kg
Power	4.9 W (average)
Bitrate	1.3 kbps
(orbit average)	
Field of view (FOV)	17° × 21°

and the energy per nucleon E/m inside the telescope. The ion's incident energy is obtained after correcting for the energy loss in the entrance foils. Table II gives the energy ranges for selected species analyzed by LEICA, and Table III lists details of the detector characteristics and geometry factor. Since LEICA measures only the mass of the ion, it cannot distinguish isobars such as ^{3}H vs. ^{3}He, or ^{40}Ar vs. ^{40}Ca. However, for the mass range of LEICA (elements $\leq$ 60 AMU) there are only a few stable isobars, and in each case one element dominates the solar system abundances (e.g., [21]) so that this is not a practical problem for the solar energetic and magnetospheric populations that LEICA detects.

Two 0.75μ Ni entrance foils separated by $\sim$ 9 mm are mounted on etched metallic grids, and give immunity to solar and geocoronal UV and visible radiation. The foils were manufactured by Lebow Co., Goleta, CA. The mounting grid is 0.010″ thick gold-plated Cu-Be, with 0.250″ square cell sizes separated by 0.005″-wide grid elements, thus achieving 96% transparency. The double entrance foils are spaced 1.0 cm apart, which prevents single pinholes from allowing sunlight to enter the telescope. The thin foils are protected by an acoustic

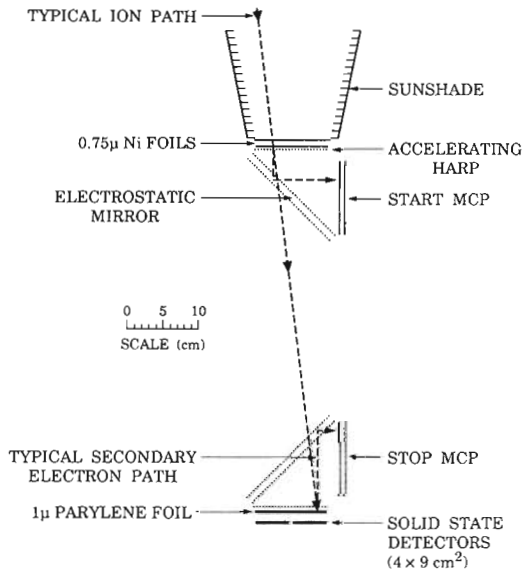

Fig. 2. Cross sectional view of the LEICA sensor. Incident ions enter through the thin foils, and pass through to one of the solid state detectors in the array at the back. The time-of-flight is determined from START and STOP pulses from microchannel plate (MCP) assemblies which are triggered by secondary electrons that are emitted from the thin foil surfaces, then accelerated and deflected by electrostatic mirrors onto the MCP surfaces.

TABLE II
LEICA ENERGY RANGES FOR SELECTED SPECIES

Species	Energy Range (MeV/nuc)	Triggering Efficiency (%)
^{1}H	>0.76	~ 1
^{4}He	0.50-6.57	6
^{12}C	0.49-10.70	64
^{16}O	0.49-8.25	67
^{20}Ne	0.46-6.79	71
^{28}Si	0.39-5.05	78
^{56}Fe	0.21-2.87	79

*measured triggering efficiency near 1 MeV/nucleon for nominal MCP bias settings; proton efficiency is estimated; Ne efficiency interpolated from other species

TABLE III
LEICA DETECTOR CHARACTERISTICS

Element	Description	Thickness (mg cm^{-2})
Outer Front Foil	0.75 μ Ni	0.668
Inner Front Foil	0.75 μ Ni	0.668
Detector foil metallic coating	0.03 μ Al	8.1×10^{-3}
Detector foil base	1 μ parylene	0.11
Detector	Geometrical Factor[1] (cm^2sr.)	Thickness and Material[2]
D1	0.13	300μ Si
D2	0.13	300μ Si
D3	0.16	300μ Si
D4	0.16	300 μ Si
Total:	0.58	

Notes: [1] Geometrical factors in this table are for *triple* coincidence (start-stop-detector) and take account of grid and harp total transmission of 73%, and details of detector and MCP alignments inside telescope

[2] the detector side through which particles enter is coated with 40 μg cm^{-2} of Au

cover (Fig. 1) that is mounted on top of the sunshade, and is opened after launch. The sunshade serves an additional role of limiting solid angle viewed by the front foil, thereby preventing excessive START rates in large solar flare events. Secondary electrons emitted from the inner Ni foil surface (see Fig. 2) are accelerated to ~ 1 kV by an electrostatic potential applied to an accelerating harp ~ 1 cm from the foil. The harp assemblies for acceleration and for the electrostatic mirrors consist of 1-mil tungsten wire strung on 1-mm spacing, thus achieving a transmission of ~ 97.5% for each layer. The use of electrostatic mirrors (e.g., [22], [23]) permits a compact design for secondary electron deflection which has the additional key features that (a) the electron flight paths from foil to MCP for normal incidence are all of the same length and therefore isochronous, and (b) an image of the foils is formed on the front of the MCP's.

The large area (7.5 × 9.3 cm active area, 1.02 mm thickness) Galileo Electro-Optics Corp. MCP's have 25 μ pore size, a channel bias angle of 19°, an open area ratio of 50%, and are mounted in a chevron arrangement. The plates are run at a low nominal bias (800 V and 850 V/plate for START and STOP, respectively) in order to prevent saturation of the position sensing electronics (see below). This low bias on the MCP's results in low overall efficiencies for ^{1}H and ^{4}He (see Table II), but for heavier species the triggering efficiency is large. The MCP bias levels are separately commandable in ~ 4V steps, and can be run at voltages up to 50% higher than nominal, allowing for adjustment post launch if the plate characteristics change. The MCP gains are monitored in flight by noting the background singles count rates of the plates; if count rates decrease noticeably, the bias is adjusted upwards to levels which produce rates comparable to the immediate post-launch values. Because of the highly variable fluxes in low earth orbit, this monitoring and adjustment is good only to a factor of ~ 2 in MCP gain. According to the manufacturer, the MCP's use recently developed glass which results in only small losses of gain vs. the total charge expelled from the plates.

The MCP outputs are directed onto thick-film anodes (manufactured by Detector Systems, Antoich, CA) deposited on alumina substrates. A solid anode on the *back* of the substrate is used to obtain the timing signal, while on the front side facing the MCP there is a wedge-and-strip anode (WSA) which is used to obtain the position of the electron cloud emerging from the MCP. The WSA electrode pattern [24], [25] is such that the analysis of signals from the three segments ("wedge", "strip", and "zigzag") of the anode allows determination of the (x, y) position of the electron cloud from the MCP. The WSA information along with the fact that the electrostatic mirrors produce images on the MCP's allows the location of the points on the Ni and parylene foils where the ion penetrated, thus permitting a determination of the flight path length L inside

the telescope. All pulse-height analyzed events are time tagged to 1-s accuracy, and since the SAMPEX pointing direction changes slowly, each event's arrival direction can be deduced off line.

In biasing of the electron emitting foils and MCP/WSA system, there is the choice of having the emitting foil at ground, and the WSA at positive 3–4 kV, or running the foil at negative 3–4 kV, and the WSA at ground (with the MCP's at appropriate intermediate biases). We obtained better results with the WSA system by running the anode at ground, thus avoiding the use of high voltage capacitors to isolate the electronics from the WSA. Thus, in Fig. 2, the inner Ni foil is biased to a nominal -2.7 kV (the outer foil is kept at ground). Similarly, we preferred keeping the solid state detector front surface at ground, and therefore the electron emitting surface for the STOP pulses is the grid mounted 1μ parylene foil with a 300Å Al coating (electron emitting surface), which was put in front of the detectors and biased at -2.7 kV.

The solid state detector array consists of four standard Ortec circular surface barrier detectors, each with 900 mm^2 active area. The light sensitivity of the solid state detectors required that the LEICA telescope be sealed, yet provision had to be made for venting during the rapid ascent on the Scout launch vehicle where the depressurization reached a maximum rate of ~ 2 lb in^{-2} s^{-1}. For the Get-Away-Special version of the instrument, air outlet vents were installed near the entrance foils; however it was found that during the Shuttle flight, the MCP's were triggered at near saturation levels. Taking account of the day/night and latitude dependencies of the count rates observed on the Shuttle flight, the best explanation for the effect was that ionospheric O^+ was entering the telescope. The O^+ density is quite large (10^5 cm^{-3}) at both Shuttle altitudes and the altitude of the SAMPEX orbit (e.g., [26]), so in the LEICA telescope all venting was through a single "chimney" which included 2 grids based at ± 40 V, which is more than sufficient to stop ions and electrons at SAMPEX altitudes.

B. Electronics

For each ion triggering the instrument, the instrument measures the time-of-flight, the energy signal in the solid state detector, and the pulse sizes from three-collector wedge-and-strip anodes (WSA) in back of both the start and stop MCP's. A triple coincidence requirement (START-STOP-Si detector) with a short ($\sim$ 350 ns) time window gives high background immunity for all analyzed events. The Si solid state detector thresholds are set at 0.5 MeV, and full scale energy deposit is 140 MeV. The primary logic and gating functions are carried out in ACTEL gate-array logic. All events triggering the system have their digitized time-of-flight and Si detector energy deposit measurements converted into pseudo-logarithmic form by fast gate logic. These $ln(t)$ and $ln(E)$ values are then used to determine whether each particle is a proton, He nucleus, or heavier than He. Events triggering LEICA that the pseudo-log lookup system identifies as protons are counted, but no further analysis is performed. Heavier nuclei are then treated as low (He) or high (heavier than He) priority for transmission to the ground. The DPU (see the accompanying article by Mabry *et al.* [27]) ensures that a sample of both priority events will be telemetered, but that low priority events will not crowd out the rarer heavy species.

Because of the very high event rates observed by LEICA in large flares, it is not possible to transmit all particle information within available telemetry allocations. Two types of information are therefore returned: first, detailed pulse-height-analysis (PHA) data at an average rate of 10 events/s, and second, counting rates which make it possible to normalize the PHA data to yield particle fluxes. In order to maximize event collection over the magnetic poles, the PHA events are read out asynchronously as described in the accompanying paper on the Data Processing Unit [28]. Table IV lists the count rates telemetered by LEICA, and Table V lists the contents of each PHA event. Those rates which count events that are analyzed by the ADC's are limited to a few thousand per second. The count rates are stored in 24-bit accumulators in LEICA, and are compressed to 12 bits by the Data Processing Unit (DPU) before telemetering the data.

Because of the low sensitivity to protons (Table II) and helium, the LEICA count rates for triple coincidences are typically very low (few counts/second) and consequently background is also very low. The singles count rates are typically highest when the spacecraft passes through the South Atlantic Anomaly, when the solid state detectors singles rates reach a few thousand per second, and the start microchannel plates count near 20 kHz. These count rates are low enough so that electronic problems such as pulse pile up are not seen with LEICA. LEICA operates in two modes: normal mode, and calibrate mode in which an internal pulser stimulates the solid state detector, time-of-flight, and WSA electronics. The calibrate mode is entered via ground command, and runs for approximately 15 minutes once per month.

C. Performance

High mass resolution analysis is done on the ground using the ion trajectory information telemetered with the PHA data. Mass histograms are formed for selected energy ranges, with the relative abundance of each species determined from the population at the appropriate mass bin in the histogram. Since LEICA has multiparameter analysis it is possible to identify and correct for residual background in the measurement, an essential feature for identifying a broad range of ions with widely differing abundances. The instrument response to heavy ions was measured prelaunch by exposing it to heavy ions beams at the Brookhaven tandem van de Graaff, and the Lawrence Berkeley Laboratory 88-inch cyclotron.

Equation (1) is used to determine the dispersions in mass resolution given the contributing dispersions in the measurement in the time of flight t, the energy deposit E, and the trajectory length L:

$$\left(\frac{\sigma_m}{m}\right)^2 = \left(\frac{\sigma_E}{E}\right)^2 + \left(2\frac{\sigma_t}{t}\right)^2 + \left(2\frac{\sigma_L}{L}\right)^2. \qquad (2)$$

We now consider each of these terms. The solid state detector energy dispersion is relatively small for particle energies above a few hundred keV/nucleon [29], [30]. As a typical value, for monoenergetic 2 MeV/nucleon ^{14}N the energy signal in the solid state detector had a measured standard deviation

TABLE IV
LEICA COUNTING RATES[1]

Name	Logic condition[2]	Type	Response	Energy Range[3]	Geometrical Factor[4] (cm^2 sr.)
D1	D1	singles discr.	All ions & electrons	> 600 keV	0.16
D2	D2	singles discr.	All ions & electrons	> 600 keV	0.16
D3	D3	singles discr.	All ions & electrons	> 600 keV	0.16
D4	D4	singles discr.	All ions & electrons	> 600 keV	0.16
START	START	singles discr.	All ions & electrons	> 250 keV (H); > 25 keV (e)	49.8
STOP	STOP	singles discr.	All ions & electrons	> 250 keV (H); > 25 keV (e)	0.73
Double Coincidence (Valid Stop)	START · STOP	logic rate	All ions	> 250 keV (H); > 25 keV (e)	0.58
Triple Coincidence (TCR)	START · STOP · $D.r$	logic rate	All ions	0.50-6.57 MeV (H)	0.58
Hi Priority	TCR · HP	ADC rate	Z> 5 ions	0.49-10.7 MeV/nuc	0.58
Lo Priority	TCR · $\overline{P}$ · $\overline{HP}$	ADC rate	He	0.50-6.57 MeV/nuc	0.58
Protons	TCR · P	ADC rate	H	>0.76 MeV/nuc	0.58
Cal Event	TCR · Cal	Internal pulser rate	not a particle rate	—	—

Notes:

[1]all counting rates are read out once every 6 seconds.

[2]notation: Dx: detector x discriminator true; HP = high priority test positive; P = proton test positive; Cal = calibrate *on*

[3]energy range shown is for most abundant species

[4]geometry factors are for singles trigger; in Table III the geometry factors are for coincidence triggers

$\sigma_E = 130$ keV. When measured in this manner, this σ_E value includes effects due to system electronics noise, solid state detector FWHM, and straggling in the Ni and parylene foils; however, in (2) the particle straggling does not enter since particles which have, e.g., higher than average losses in the Ni foils, will also have longer times of flight which compensate and therefore don't increase the dispersion. Thus, the value $\sigma_E = 130$ keV is an upper limit. The contributions to this σ_E from system noise is independent of species and energy, and the contribution from the detector FWHM is independent of energy for each species above ~ 100 keV/nucleon.

The dispersion in the time-of-flight in (2) is due primarily to "walk" in the time-to-amplitude converter which occurs when different START and STOP signal sizes trigger the system. The effect is particularly important in systems using MCP's since these plates show a broad FWHM signal size even for heavy ions of the same energy. In the LEICA design, constant fraction discriminators compensate for most of the time-of-flight "walk". In order to estimate the time-of-flight dispersion in the system, we exposed the instrument to a "monoenergetic" ^{28}Si beam at 4.2 MeV/nucleon, and measured a time-of-flight dispersion $\sigma_t = 330$ ps. For particles at this high an energy, energy losses in the thin foils are small, and so energy straggling is also very small; thus, the time-of-flight dispersion for these particles is presumably a measure of dispersions in the electronics, mirror system, etc., and is the same for particles of different energies. Thus, we can use this result to estimate the time dispersion for ~ 1 MeV per nucleon ions; since their the flight time in the telescope is ~ 45 ns, a 330 ps dispersion leads to $\sigma_t/t = 0.007$ in this case.

TABLE V
LEICA PULSE HEIGHT EVENT CONTENTS

Item	Number of Bits
Solid State Detector	12
Time-of-flight	12
START Wedge	12
START Strip	12
START Zigzag	12
STOP Wedge	12
STOP Strip	12
STOP Zigzag	12
Time of day[1]	16
FLAGS:	
Calibrate enable	1
Hi Priority	1
Calibrate event	1
D1 triggered	1
D2 triggered	1
D3 triggered	1
D4 triggered	1
Multiple START pulses	1
Total:	120

Notes: [1]Hour, min, sec

The $\Delta L/L$ term in (2) is derived from the accuracy of the WSA position sensing system, evaluated in terms of the related uncertainty in the particle path length L (~ 50 cm) in the telescope. The MCP/WSA system returns accurate information ($\sigma < 0.2$ mm) information on the location of the secondary

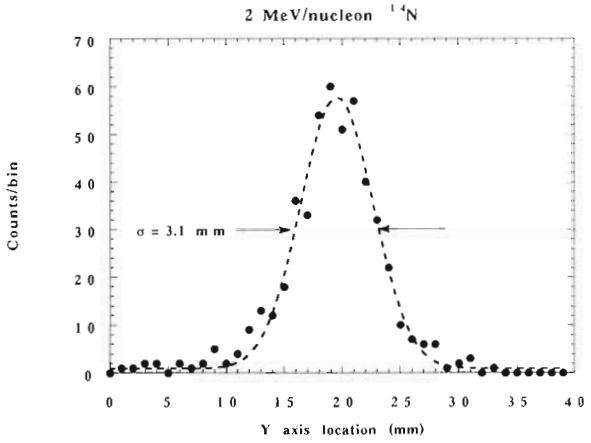

Fig. 3. "Spot" size on the front MCP from a 1-mm diameter beam spot of 2 MeV/nucleon ^{14}N incident on the front foil. The spread of secondary electron emission angles with respect to the foil surface dominates the width of the spot.

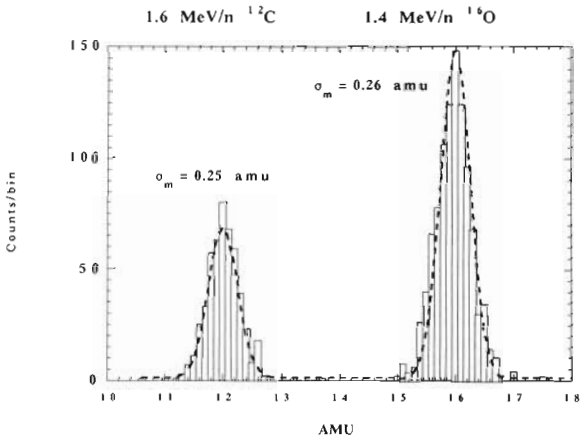

Fig. 4. Mass histograms of ~ 1.5 MeV/nucleon ^{12}C and ^{16}O.

electron impact sites on the front of the MCP. However, the knowledge of where the ions penetrated the foil is less accurate than this because the secondary electron emission angle with respect to the surface normal follows a cosine distribution [31]. Propagated through the LEICA mirror system, the result is that electrons leaving the foil from a single spot may land anywhere within a ~ 1 cm diameter circle on the MCP's. There may be additional effects introduced by the mirrors since their electrostatic fields are not perfectly uniform. For heavy ions, the large numbers (10 s, e.g., [32]) of secondary electrons should compensate for this somewhat since for such events there are multiple electrons hitting the MCP and the spatial dispersions should tend to cancel out. Fig. 3 shows the measured spot size for ~ 2 MeV/nucleon ^{14}N which was collimated to strike the START incident foil through a 1 mm diameter hole. The standard deviation of the distribution is 3.1 mm; combining this uncertainty in both x and y directions for both the START and STOP MCP's, the weighted average uncertainty in the total path length L between the foils is $\Delta L/L = 0.0006$. With these values of the various dispersions, we may estimate the mass resolution for 1.4 MeV/nucleon ^{12}C: after penetrating the foils, this ion deposits 13 MeV in the solid state detector, and has a flight time of 35.5 ns thus:

$$\left(\frac{\sigma_m}{m}\right)^2 = \left(\frac{0.13}{13}\right)^2 + \left(2 \times \frac{.33}{35.5}\right)^2 + (2 \times 0.0006)^2 \quad (3)$$

so

$$\frac{\sigma_m}{m} = 0.021 \quad (4)$$

and

$$\sigma_m = 0.25\, AMU$$

in reasonable agreement with the measured mass resolution shown in Fig. 4.

D. Data Products

Routine data products from LEICA are generated by combining the counting rate and pulse height data to give absolute fluxes and energy spectra of different species. In addition to the calibration and triggering efficiencies mentioned above, it is also necessary to correct for coulomb scattering in the Ni foils in order to recover incident flux levels. This effect is important only below ~ 1 MeV/nucleon.

Time-intensity profile plots are generated on an orbit by orbit basis, and over longer time periods (1 week, 1 month) for studies of longer-lasting events such as large solar flares. Longer time period studies related to solar flare events consist of data taken only at geomagnetic latitudes high enough to be essentially free of distortion from cutoff effects. Short events such as precipitating magnetospheric heavy ions are identified on the orbit plots and then analyzed in detail on high time resolution displays. High mass resolution analyses such as shown in Fig. 4 are done only for periods selected for their interest in solar flare or magnetospheric studies.

ACKNOWLEDGMENT

The construction, testing, and calibration of the LEICA instrument was carried out by the Space Physics group of the Department of Physics. We particularly thank E. Tums, R. Pappalardo, S. Graham, P. Floros, S. Lasley, R. Lundgren, M. Pairel, H. Wats, P. Ipavich, and A. Desrosier for their contributions to the design, construction, and administrative management of the project. The LEICA instrument was constructed under NASA contract NAS5-30704, with key instrument concepts developed under instrumentation grant NAGW-1990.

REFERENCES

[1] G. M. Mason and G. Gloeckler, "A Supra-thermal energetic particle detector (STEP) for composition measurements in the range ~ 20 keV/nucleon to 1 MeV/nucleon," *Proc. 17th Internat. Cosmic Ray Conf., (Paris)*, vol. 8, p. 98, 1981.

[2] D. V. Reames, T. T. von Rosenvinge, R. Ramaty, G. M. Mason, D. C. Hamilton, M. A. Forman, and W. R. Webber, "The energetic particles: acceleration, composition and transport (EPACT) experiment on the ISTP/Wind spacecraft," in *Particle Astrophysics: the NASA cosmic ray program for the 1990s and beyond, A.I.P. Conf. Proc. No. 203*, W. V. Jones, F. J. Kerr, and J. F. Ormes, Eds. New York: A.I.P., p. 32.

[3] B. Klecker, D. Hovestadt, M. Scholer, H. Arbinger, M. Ertl, H. Kästle, E. Künneth, P. Lawverenz, E. Seidenschwang, J. B. Blake, N. Katz, and D.

Mabry, "HILT: a heavy ion large area proportional counter telescope for solar an anomalous cosmic rays," *IEEE Trans. Geosci. Remote Sensing*, vol. 31, pp. 542–548, May 1993.
[4] D. Hovestadt, B. Klecker, P. Laeverenz, E. Seidenschwang, G. M. Mason, P. D. Bedini, G. Gloeckler, D. C. Hamilton, J. B. Blake, and D. Chenette, "Experiment for charge determination of cosmic rays of interplanetary and solar origin on the space shuttle," *Proc. 20th Internat. Cosmic Ray Conf., (Moscow)*, vol. 4, p. 406, 1987.
[5] G. M. Mason, J. E. Mazur, P. H. Walpole, T. L. James, and T. R. Sharp, "Report on the University of Maryland Large Area Telescope (LAT) flight on the Space Shuttle Columbia STS-28, August 1989," Univ. of Maryland, Dept. of Physics, Preprint 91-126, 1990.
[6] G. M. Mason, G. Gloeckler, and D. Hovestadt, "Temporal variations of nucleonic abundances in solar flare events. II. Evidence for large-scale shock acceleration," *Astrophys. J.*, vol. 280, p. 902, 1984.
[7] H. V. Cane, D. V. Reames, and T. T. von Rosenvinge, "The role of interplanetary shocks in the longitude distribution of solar energetic particles," *J. Geophys. Res.*, vol. 93, p. 9555, 1988.
[8] D. V. Reames, T. T. von Rosenvinge, and R. P. Lin, "Solar ^{3}He-rich events and nonrelativistic electrons: a new association," *Astrophys. J.*, vol. 292, p. 716, 1985.
[9] G. M. Mason, D. V. Reames, B. Klecker, D. Hovestadt, and T. T. von Rosenvinge, "The heavy ion compositional signature in ^{3}He-rich solar particle events," *Astrophys. J.*, vol. 303, p. 849, 1986.
[10] G. M. Mason, "The composition of galactic cosmic rays and solar energetic particles," *Rev. Geophys.*, vol. 25, p. 685, 1987.
[11] R. P. Lin, "Solar particle acceleration and propagation," *Rev. Geophys.*, vol. 25, p. 676, 1987.
[12] D. V. Reames, "Energetic particles from impulsive solar flares," *Astrophys. J. Suppl.*, vol. 73, p. 235, 1990.
[13] W. R. Cook *et al.*, "MAST: A mass spectrometer telescope for studies of the isotopic composition of solar, anomalous, and galactic cosmic ray nuclei," *IEEE Trans. Geosci. Remote Sensing*, vol. 31, pp. 557–564, 1993.
[14] J. A. Van Allen, B. A. Randall, and S. M. Krimigis, "Energetic carbon, nitrogen, and oxygen nuclei in the earth's outer radiation zone," *J. Geophys. Res.*, vol. 75, p. 6085, 1970.
[15] J. Moritz, "Energetic protons at low equatorial altitudes: A newly discovered radiation belt phenomenon and its explanation," *Zeit. Geophys.*, vol. 38, p. 701, 1972.
[16] D. Hovestadt, B. Hausler, and M. Scholer, "Observations of energetic particles at very low altitudes near the geomagnetic equator," *Phys. Rev. Lett.*, vol. 28, p. 1340, 1972.
[17] P. F. Mizera, and J. B. Blake, "Observations of ring current protons at low altitudes," *J. Geophys. Res.*, vol. 78, p. 1058, 1973.
[18] J. B. Blake, "On the ionic identity of the ring current particles," *J. Geophys. Res.*, vol. 81, p. 6189, 1976.
[19] M. Scholer, D. Hovestadt, G. Hartmann, J. B. Blake, J. F. Fennell, and G. Gloeckler, "Low-altitude measurements of precipitating protons, alpha particles, and heavy ions during the geomagnetic storm on March 26–27, 1976," *J. Geophys. Res.*, vol. 84, p. 79, 1979.
[20] H. K. Rassoul, R. P. Rohrbaugh, and B. A. Tinsley, "Low-altitude particle precipitation and associated local magnetic disturbances," *J. Geophys. Res.*, vol. 97, p. 4041, 1992.
[21] E. Anders, and M. Ebihara, "Solar-system abundances of the elements," *Geochim. et. Cosmochim. Acta*, vol. 46, p. 2363, 1982.
[22] F. Busch, W. Pfeffer, B. Kohlmeyer, D. Schüll, and F. Pühlhoffer, "A position-sensitive transmission time detector," *Nucl. Instr. and Method.*, vol. 171, p. 71, 1980.
[23] W. Starzecki, A. M. Stefanini, S. Lunardi, and C. Signorini, "A compact time-zero detector for mass identification of heavy ions," *Nucl. Instr. and Method*, vol. 193, p. 499, 1982.
[24] O. H. W. Siegmund, R. F. Malina, K. Coburn, and D. Werthimer, "Microchannel plate EUV detectors for the Extreme Ultraviolet Explorer," *IEEE Trans. Nuc. Sci.*, vol. NS-31, p. 776, 1984.
[25] J. S. Lapington and H. E. Schwarz, "The design and manufacture of wedge and strip anodes," *IEEE Trans. Nuc. Sci.*, vol. 33, p. 288, 1986.
[26] J. Kelley, in *The Earth's Ionosphere*. (International Geophysics Series, vol. 43). New York: Academic Press, 1981, p. 192.
[27] D. J. Mabry, S. J. Hansel, and J. B. Blake, "The SAMPEX data processing unit (DPU)," *IEEE Trans. Geosci. Remote Sensing*, vol. 31, pp. 572–574, May 1993.
[28] ibid.
[29] A. B. Galvin, "Charge states of heavy ions in the energy range ~ 30–130 keV/Q observed in upstream events associated with the earth's bow shock," Ph.D. thesis, University of Maryland, Department of Physics, preprint 82-214, p. 250, 1982
[30] E. D. Klema, F. J. Camelio, and T. K. Saylor, "Energy resolution of silicon surface-barrier detectors for oxygen and sulfur ions," *Nuc. Instr. and Methods.*, vol. 225, p. 72, 1982.
[31] W. Meckbach, "Secondary electron emission from foils traversed by ion beams," in *Beam-Foil Spectroscopy*, (vol. 2), I. A. Sellin and D. J. Pegg, Eds. New York: Plenum Press, 1976, p. 577; see also: H. Stolz, *Ann. Phys.*, vol. 3, p. 196, 1956.
[32] D. Hasselkamp, K. G. Lang, A. Scharmann, and N. Stiller, "Ion induced electron emission from metal surfaces," *Nucl. Instr. and Method.*, vol. 180, p. 349, 1981.

Glenn M. Mason, for a photograph and biography, please see page 541 of this issue.

Douglas C. Hamilton received the B.A. degree in physics and mathematics from the University of Kansas and the Ph.D. degree in physics from the University of Chicago.

He came to the University of Maryland in 1978 and is now Associate Professor in the Department of Physics. His research has concentrated on particle composition, acceleration, and transport in planetary magnetospheres and interplanetary space. He is a Co-investigator on NASA SAMPEX, ISTP, Voyager, and AMPTE missions.

Peter H. Walpole received the B.A. degree in physics from the University of Chicago, where he also took graduate courses in physics.

He came to the University of Maryland in 1978, and was Senior Electronics Engineer for the LEICA instrument. Previously he served an engineer for experiments on Pioneer 10, 11, Mariner 10, ISEE-3, AMPTE, Get-Away-Special and ULYSSES missions.

Karl F. Heuerman received the B.S. and M.S. degrees in physics from Miami University, Ohio.

He joined the University of Maryland Space Physics Group in 1990. He carried out LEICA sensor development, testing, and calibration.

Tommy L. James joined the Space Physics group as Mechanical Designer in 1978, and was responsible for LEICA detailed mechanical design and fabrication. While at Maryland Tom has also worked energetic particle sensor designs on the ULYSSES, AMPTE and Get-Away-Special programs.

Michael H. Lennard received the B.S. degree in electrical engineering from the University of Maryland College Park.

He joined the University of Maryland Space Physics Group in 1990 and designed and tested the LEICA digital electronics; after the instrument was constructed, Mike wrote the basic data capture and processing programs for the SAMPEX Science Operations Center.

Joseph E. Mazur received the B.A. degree in physics from the University of Chicago in 1985 and the Ph.D. degree in physics from the University of Maryland in 1991.

He is now a research associate at the University of Maryland studying flare particle acceleration and composition.